Journal of Ocean Engineering and Marine Energy (2022) 8:573–585
https://doi.org/10.1007/s40722-022-00256-9

RESEARCH ARTICLE

Ship hydrodynamics knowhow derived from computational tools: some examples

Hoyte C. Raven[1]

Received: 30 April 2022 / Accepted: 3 August 2022 / Published online: 4 September 2022

Abstract
This paper discusses how the use of today's computational tools can lead to a quick advance of the field of ship hydrodynamics, by answering long existing questions, indicating simple models and demonstrating design trends. Some examples are given of subjects for which analysis of computational results, from RANS and free-surface potential flow codes, has led to improved understanding of the flow. The first example describes how better understanding of ship wave making and its dependence on the hull form has been obtained from analysis of potential flow calculations. The resulting insight is still used in the context of CFD-based hull form optimisation. The second example describes how questions regarding the model-to-ship extrapolation of experimental results have been solved using RANS computations. The last example shows how computational study of shallow-water effects has led to a method to correct for tank width effects in model measurements; to an improved model-to-ship extrapolation procedure for shallow water tests; and to a simple trial correction method for moderate shallow-water effects. The examples are meant to illustrate and promote this sort of research, and subjects are mentioned for which similar progress can probably be made using CFD methods.

Keywords CFD · Ship wave making · Shallow water · Model-to-ship extrapolation

1 Introduction

Ship hydrodynamics is a field of science with a respectable history. The oldest towing tanks were built in the eighteenth century, and the Froude hypothesis underlying all model testing work dates from 1868. Important empirical knowledge has been built up over time. Predictions of ship full-scale performance were, and usually are, typically based on model tests, using model-to-ship extrapolation procedures based on empirical knowledge and a large database of full-scale correlation data. Ship hull form design was classically done by experienced designers, using their knowledge and empirical insights in the flow physics determining resistance and propulsion.

Today, CFD predictions play an increasing role in the design process. More and more complete and accurate computations are made. But prediction alone does not lead to a better ship. Insight in the flow physics remains essential if we are to design more efficient ships. Furthermore, basing the final full-scale performance prediction just on CFD computations for the self-propelled ship is not considered sufficiently reliable yet; therefore, model testing still is a standard component for larger ships.

A smooth transition from the empirical to a computational process, and continuous improvement of design quality, can best be guaranteed by a good integration of the two approaches. On one hand, this means that CFD predictions cannot simply replace those based on model tests, unless with much attention for modelling and numerical accuracy, full-scale validation and determination of correlation data; and that CFD-based design and optimisation should exploit existing knowledge of the flow physics and design trends. On the other hand, today's computational methods offer unprecedented possibilities for extending our insight in the flow around the hull, scale effects and design trends. Quick progress beyond the classical knowledge can be made; e.g. by analysing computed flow fields and pressure distributions, by performing scale effect studies and integrating CFD use in the power prediction based on model tests, or by CFD-based optimisation leading possibly to new design solutions.

✉ Hoyte C. Raven
raven032@planet.nl

[1] Maritime Research Institute Netherlands (MARIN), P.O. Box 28, 6700AA Wageningen, Netherlands

The present paper will discuss some examples of how computational methods have contributed to ship hydrodynamics knowhow. All are taken from the author's research at MARIN over the years; not to present latest results but to illustrate and propagate this use of computational tools and, hopefully, provide inspiration to others. The CFD work is unspectacular, but the computational results still have enabled to obtain most practical insights and identify simplified models that help understanding mechanisms and trends.

2 Understanding and reducing ship wave making

2.1 Early theoretical developments

The first example we are considering is, how computations have contributed to the insight in the mechanism of ship wave making and to the effectivity of wave resistance minimisation.

Early theoretical developments on ship wave making were based on analytical methods for potential flow. Until around 1965, this mostly concerned methods in which not only the free-surface boundary conditions were linearised, but also the hull boundary condition. Thin-ship, flat-ship and slender-ship approximations have been derived and studied. Neither of these was applied widely and successfully in ship hull form design, because of the large deviations of the calculated resistance for real ships. While the insights derived on the properties of ship wave patterns are still essential knowledge today, the approximations made precluded learning much about the relation with the hull form. For design, rather the guidelines from systematic series of model tests were used, along with simple theories regarding interference, as proposed by Wigley.

With the introduction of bulbous bows, attempts have been made to understand their action from the available theories, but with little success. In practice, designing and optimising a bulbous bow was a matter of 'trial and error', through many model tests with modifications of the model shape. Semi-theoretical approaches have been tried to find the best bulb size and longitudinal position based on just few experiments (Sharma and Naegle 1970), but no indication was thus found of the desired bulbous bow *shape*.

Around 1970–1975, 'slow-ship linearised' free-surface methods were being proposed, in which the free-surface boundary condition was linearised relative to double-body flow but the true hull boundary condition was imposed. There has been some debate on their formulation (e.g. Newman 1976), and evaluating these theories numerically was a challenge at that time. But Dawson's method (1977) did provide a practical formulation permitting efficient computation. At MARIN, we started using this method in practice from 1987 (Raven 1988). Like several others we found that quite puzzling results could be obtained for wave resistance. The subsequent development of nonlinear free-surface panel methods (Jensen 1988; Raven 1992, 1996; Janson 1997) led to a much better generality and accuracy, removing the main shortcomings of the wave resistance prediction. It is this class of methods that permitted a widespread use in practical ship design. At MARIN, the code RAPID (Raven 1996) is in uninterrupted practical use since 1994.

2.2 The mechanism of wave making

At least with panel densities computationally feasible in the 1990's, the numerical accuracy of the wave resistance prediction was still a problem. But the predicted flow field was in good agreement with reality. For us, a breakthrough came when we found a way to derive insights on desired hull form modifications from the computed flow field and wave pattern, rather than just trying to reduce wave resistance by trial and error. A combined visualisation of wave pattern, hull form, pressure distribution and streamline direction was not usual in those days, but became available and helped a lot in analysing the computed fields. The hull pressure distribution in particular, which is hardly feasible to measure in a model test, proved to be an essential result.

Through analyses of many calculated results and tentative hull form adjustments, insight in the wave-making mechanism was obtained. This was later more formally described (Raven 2010; Larsson and Raven 2010) as a procedure that conceptually splits the relation of a hull form and the wave pattern it generates, into two steps:

1. The relation of a hull form and the pressure distribution on the hull and still-water surface it generates;
2. The wave pattern generated by that pressure distribution.

While the steps are not disjunct and the second step does affect the first, for the not too high Froude numbers typical of conventional ships this is fairly limited. The advantage of the separation into two steps is that each of them follows some rather straightforward rules, very briefly summarised as follows:

1. Hull form to hull pressure distribution: This is dominated by streamline curvatures; so, by the hull surface curvature in the streamline direction, and also by the streamwise slope of the hull surface (as that affects streamline curvature at a distance).
   Hull pressure distribution to pressure distribution on still-water surface: This is determined by the ratio of the length scale of the features of the hull pressure distribution, to their distance to the still-water surface. If that ratio is large (e.g. a large-scale pressure variation close to the surface),

that pressure disturbance is felt at the surface without much change. If the ratio is small (e.g. a short pressure variation further beneath the surface), the hull pressure feature is felt at the free surface as a much reduced pressure variation with larger length scale.

2. Surface pressure distribution to wave pattern: the wave components preferentially generated by a surface pressure distribution are those that have a length scale and shape comparable to that of the pressure distribution; longitudinally and transversely.

These steps are of course nothing revolutionary. The second step is well approximated by an analytical expression from linear theory, known since a century, but its use in the present context was not common. The meaning of the second step can easily be illustrated by the wave patterns generated by a free-surface pressure distribution moving over the water surface with speed V (Raven 2010). In Fig. 1, the pressure imposed on the surface has a sinusoidal shape lengthwise, constant crosswise, and has equal amplitude in all figures. In the first three figures its width is $\lambda_0 = 2\pi V^2/g$. In the first figure, the length is 2 λ_0, so it does not fit any steady wave—wave making is quite limited. In the second figure, the length is λ_0, fitting a transverse wave perfectly. A dominant transverse wave is generated, causing much wave resistance. In the third figure, the pressure patch length is halved again, to $\lambda_0/2$; it does not fit a transverse wave well, which, therefore, is reduced; but it does fit a diverging wave. However, the width of the pressure patch leads to the generation of two sets of diverging waves, plus some transverse waves. If now, we also halve the width of the pressure distribution to $\lambda_0/2$, the pattern is entirely dominated by diverging waves. The figures show how the wave pattern is entirely determined by the length scales of the pressure distribution. From linear theory, this applies to all components of an arbitrary pressure distribution containing various length scales.

Owing to the conceptual distinction of the two steps, these considerations apply as well to components of the pressure distribution induced by the ship. While nonlinear effects and propagation over the curved near-field flow do modify wave amplitudes and directions, still the linear relations dominate the wave pattern, and thereby give useful qualitative information on the cause of wave components and measures to reduce them.

We note that the idea of this two-step approximation of ship wave making is already described in Lighthill (1980),

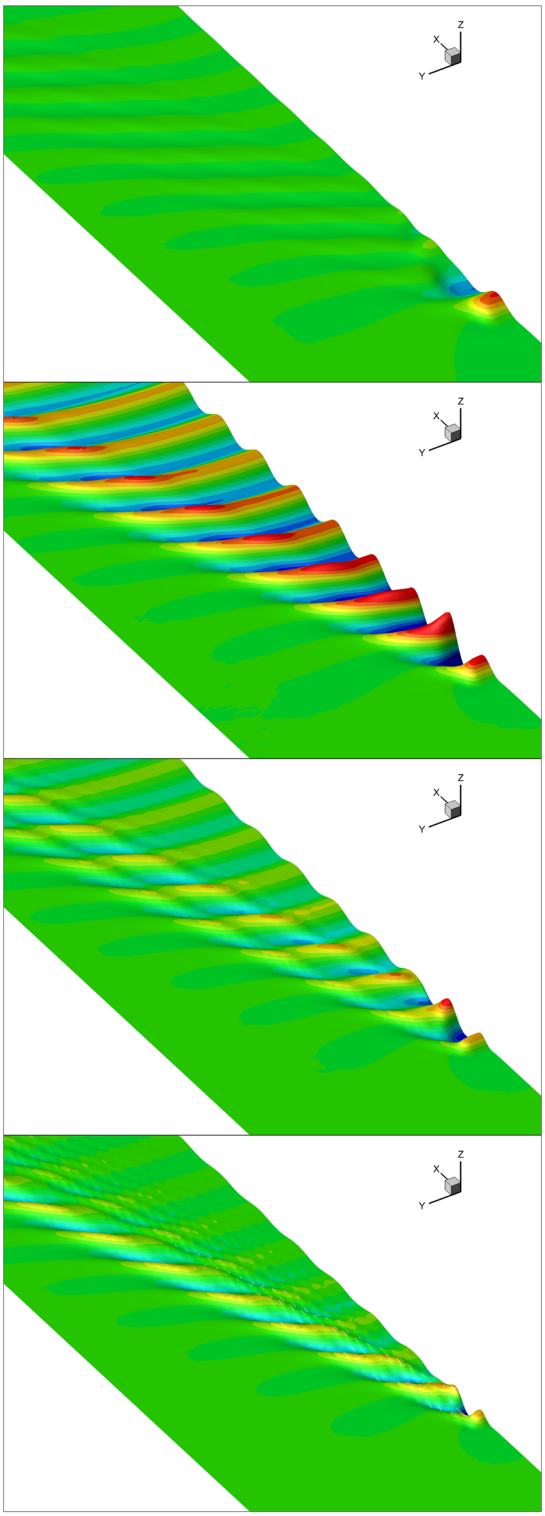

Fig. 1 Waves generated by a pressure patch travelling over the free surface. Top to bottom: patch width λ_0 and patch length 2 λ_0, λ_0, and 0.5 λ_0, respectively; and patch width 0.5 λ_0, patch length 0.5 λ_0

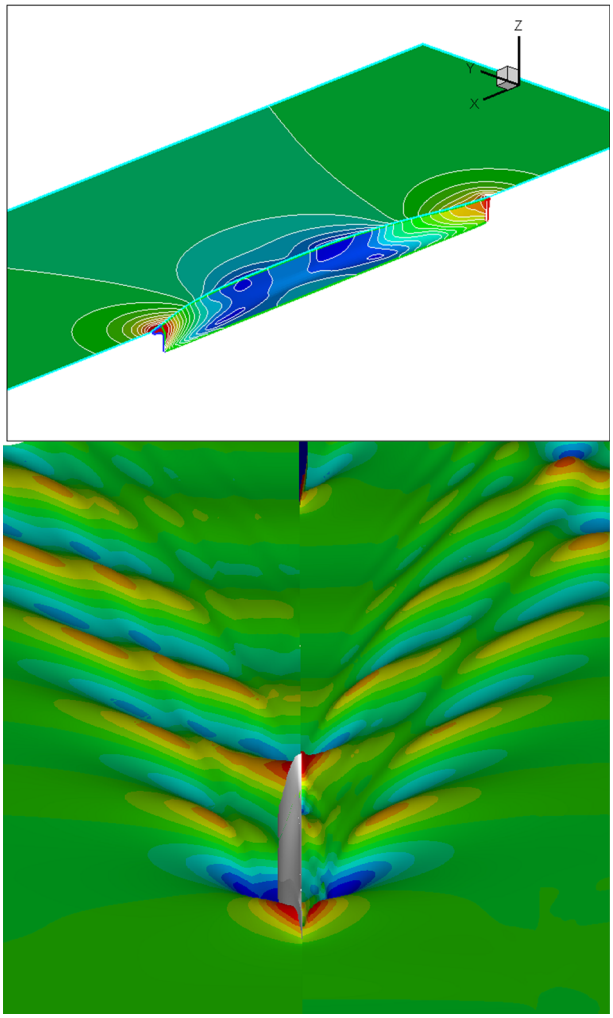

Fig. 2 A check of the two-step procedure, for Series 60 $Cb = 0.60$ ship at $Fr = 0.316$. Top: double-body pressure distribution on hull and still-water surface, Bottom: right side: wave pattern generated by minus this double-body pressure distribution in absence of the hull. Left side: Wave pattern of the same hull, computed by RAPID

without any reference or validation, and is used to discuss the action of a bulbous bow. Therefore, the components of this procedure were there but the application in design appeared essentially unknown.

To assess the usefulness of this two-step consideration for practical cases, in Raven (2010), a strict computational equivalent was set up: first, the still-water pressure distribution generated by the hull in double-body flow was computed; next, the wave pattern generated by minus that pressure distribution imposed on the free surface was calculated, in absence of the hull. This corresponds essentially with an older slow-ship linearised theory by Baba and Takekuma (1975). Figure 2 shows that the wave pattern for the Series 60 $Cb = 0.60$ hull as found from that simple method corresponds fairly well with that of a full nonlinear potential flow calculation, thus supporting the qualitative validity of this two-step analysis approach; not for prediction, but for understanding. The same was found for various other cases.

As discussed in Larsson and Raven (2010), the qualitative guidelines for both steps explain much of what is known and observed on ship wave patterns. Both steps are simple enough to be easily estimated and understood. The disregard of near-field effects and nonlinearities hardly matters for their practicality as long as we remain aware of those. The simple analysis procedure, which at MARIN, we use since around 1990, still plays an important role in our ship design work. We use it, informally, to understand a computed wave pattern; and to decide what hull form modifications to make for eliminating the dominant wave components. Frequently, significant improvements can thus be made in a few directed steps.

2.3 Systematic variations and optimisation

A new dimension of this possibility to investigate and understand the dependence of the flow and wave pattern on hull form features came with the development of a visualiser for computations for parametric hull form variations. Figure 3 is a screenshot of the user interface. Here we consider a three-parameter variation of the bulbous-bow shape. Free-surface potential flow computations have been done using RAPID, for a set of $5 \times 5 \times 5$ hull forms of this family. In the visualiser, the hull form can be varied by moving the sliders top right, and the tool interpolates the flow data in the underlying set of flow solutions for whatever combination of the three parameters requested. The wave pattern, flow direction and pressure distribution for continuous variation of the hull form parameters are thus instantly shown. This tool gives an unprecedented insight in the detailed design trends and the mechanisms determining the flow and wave making. Contrary to a usual optimisation, we do not just obtain the trend of the objective function, e.g. resistance, but also how this is related to changes of the flow field.

This visualiser was initially developed for potential flow results, and later extended for free-surface viscous-flow computations using the PARNASSOS code. Figure 4 illustrates its use for inspection of limiting streamlines on the stern and nominal wake field dependent on hull form parameters (Raven 2014).

The same insights still serve in the context of a formal computational optimisation of ship hull forms. Many publications appear in which hull forms are optimised for minimal wave resistance, using a set of parameters just selected from geometric considerations. In that way, no use is made of the existing knowledge on ship wave making and the insights developed in the past, and the process may become needlessly expensive computationally. Instead, for minimising wave resistance, we select parametric deformations of an

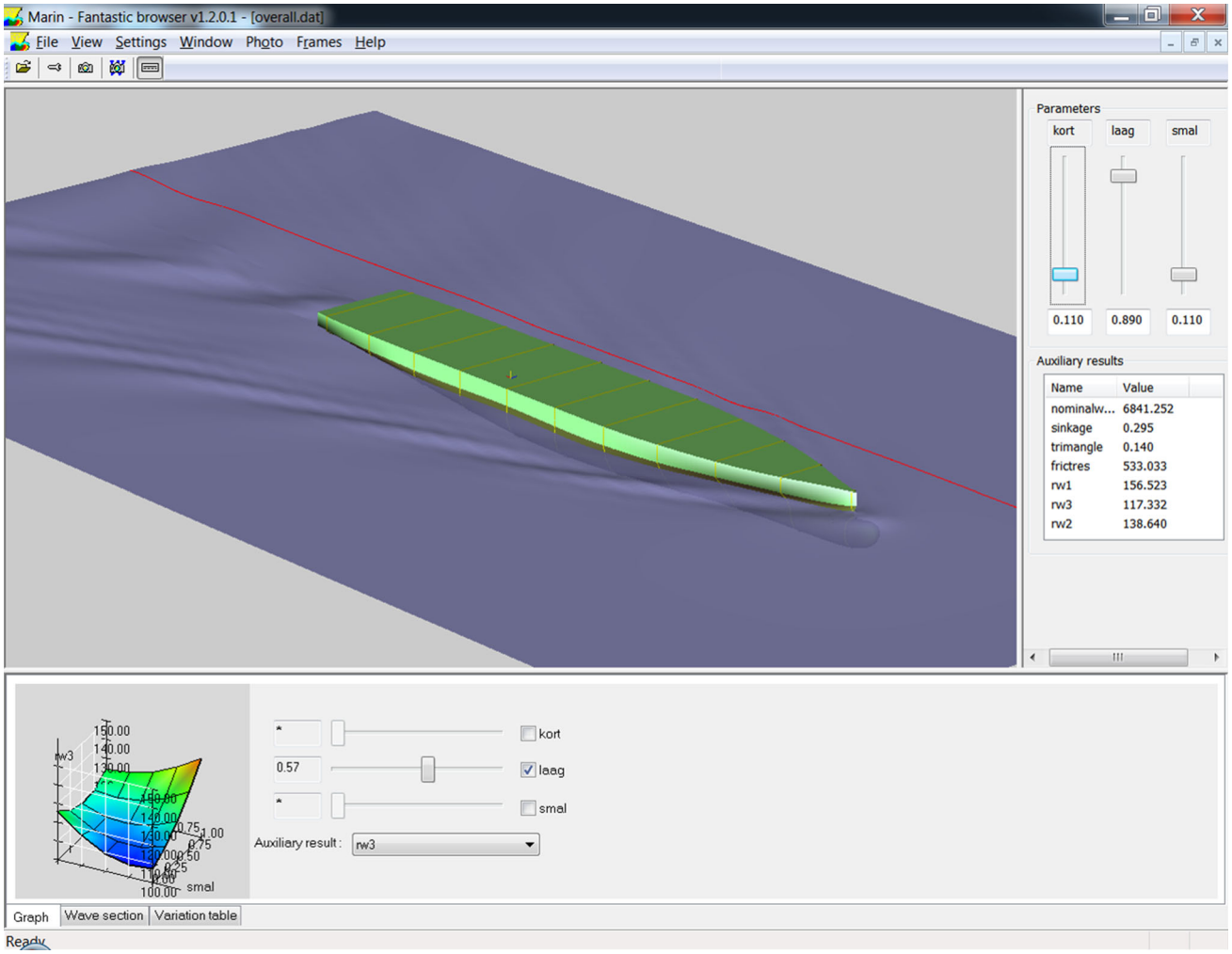

Fig. 3 Visualiser for flow fields of systematically varied hull forms. Wave pattern, from free-surface potential flow code, for three-parameter bulbous bow variation

initial hull form based on the same hydrodynamic considerations: we aim at using a set of hull form parameters that directly address the dominant wave components of the initial hull form. In this way, with a limited set of parameters significant improvements can often be achieved (Raven and Scholcz 2017).

Thus, this example illustrates how close inspection of systematic, or also unsystematic, computational results can provide information and insights unreachable otherwise. Existing linear theories provided the proper background to develop the simplified model of ship wave making and insight in design trends. The model and its proper use only became apparent from computational results, in this case from a free-surface potential flow code. The availability of calculated hull pressure distributions along with the wave patterns has been instrumental in understanding and, in a way, demystifying, ship wave making.

3 Scale effects on ship resistance

3.1 Model-to-ship extrapolation

As a next example of a field where CFD computations have provided essential information, we consider resistance scale effects. To predict the resistance of a ship based on model tests, the Froude hypothesis is used, which, in modern terms, approximates the resistance coefficient as the sum of a viscous resistance just dependent on the Reynolds number, and a wave resistance just dependent on the Froude number:

$$Ct(\mathrm{Fr},\ \mathrm{Re}) = Cv(\mathrm{Re}) + Cw(\mathrm{Fr}). \tag{1}$$

From a model test, the ship resistance coefficient at equal Froude number is then calculated by correcting for the dif-

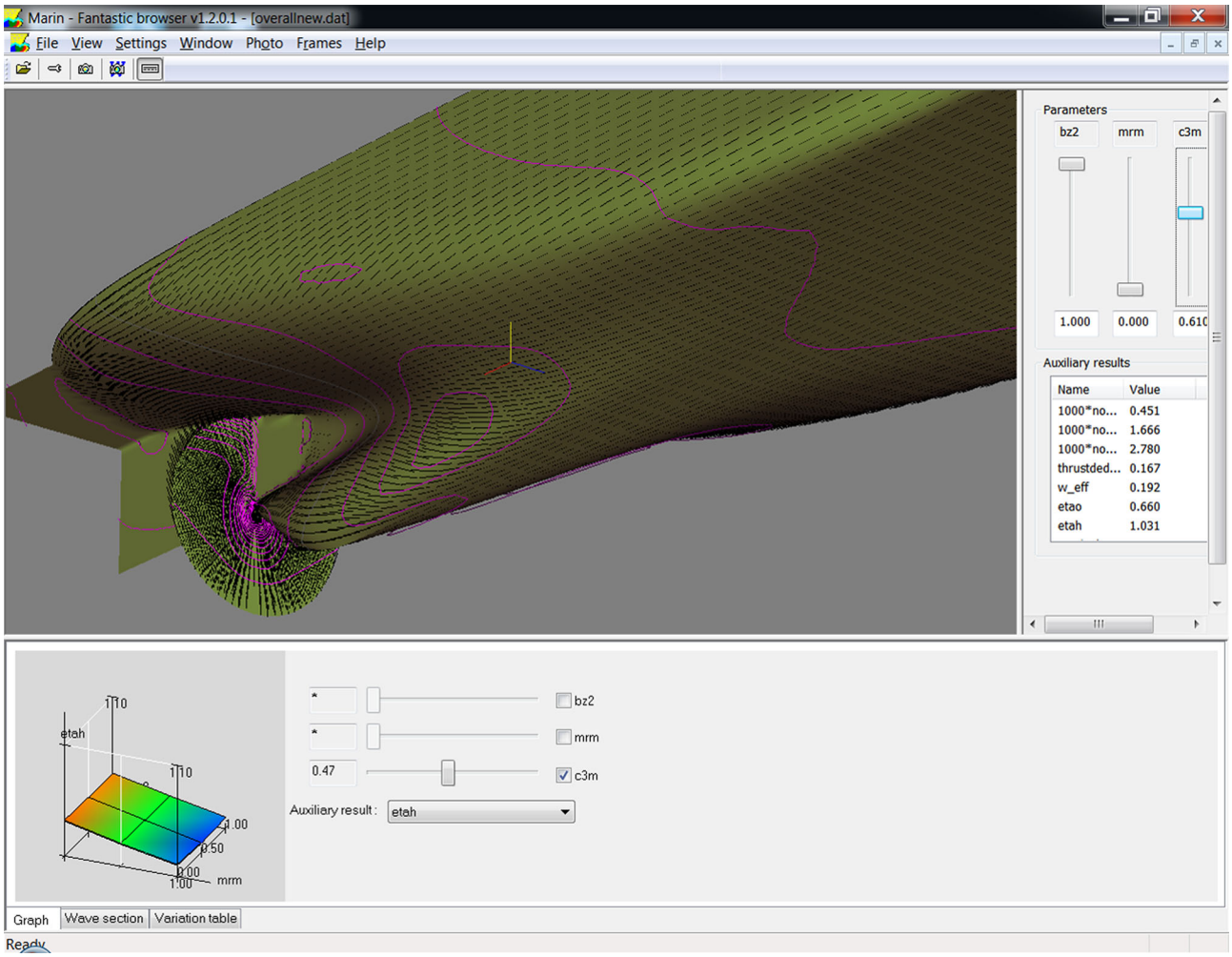

Fig. 4 Visualiser for flow fields of systematically varied hull forms. Limiting streamline directions and wake field, from RANS code PARNASSOS, for three-parameter stern variations

ference in viscous resistance coefficient resulting from the difference between the ship Reynolds number (Re_s) and that of the model (Re_m):

$$Ct(\mathrm{Fr}, \mathrm{Re}_S) = Ct(\mathrm{Fr}, \mathrm{Re}_M) - Cv(\mathrm{Re}_M) + Cv(\mathrm{Re}_S). \quad (2)$$

In the usual model-to-ship extrapolation, the viscous resistance coefficients are supposed to be proportional to the frictional resistance coefficients of a flat plate at equal Re:

$$Cv(\mathrm{Re}) = (1 + k)Cf_0(\mathrm{Re}). \quad (3)$$

Therefore, the form factor $1 + k$ is supposed to be equal for model and ship. This supposition has sometimes been doubted; at least for fuller hull forms. But until the availability of accurate CFD, there was no way to validate it. Geosim testing (testing geometrically similar models at several scales) just covers a most limited part of the required range of Reynolds numbers. Full-scale trials only provide measured propulsion power and RPM for a given speed, and any link to a viscous resistance scale effect is most indirect.

3.2 Computational scale effect studies

Instead, computing form factors using CFD is in principle straightforward. We just calculate the 'double-body flow', the flow around the underwater part of the ship with the still-water surface represented as a symmetry plane. Wave making is thus excluded and the resistance found is purely viscous, properly representing the limit for Fr $\rightarrow$ 0. Dividing it by the frictional resistance coefficient of a flat plate at equal Re, taken from a 'plate friction line', directly provides the form factor. If we do this for model and full scale, we can check whether the form factor is equal for both.

However, we note here that for quite some time, very few full-scale computations using RANS codes were published. For most CFD codes, a stable and converged computation for full-scale Re with $y^+ < 1$ was unachievable for a long time,

Table 1 Calculated form factors for 'Hamburg Test Case' with different plate friction lines

Plate friction line	$1+k$ model	$1+k$ ship	Difference (%)
ITTC'57	1.138	1.222	7.4
Schoenherr	1.161	1.221	5.2
Grigson	1.154	1.157	0.3
Katsui	1.179	1.202	2.0
Numerical friction line	1.213	1.227	1.2

and still seems not feasible for some codes. Avoidance of this problem by using wall functions has the significant disadvantage of possibly distorting the scale effects found. Probably the first paper on full-scale ship viscous-flow computations without wall functions was (Eça and Hoekstra 1996). The RANS code used, PARNASSOS (Hoekstra 1999; Van der Ploeg et al. 2000) is a proprietary code from MARIN and IST Lisbon, dedicated to computation of the flow around ship hulls. It is a multiblock structured-grid finite-difference method, and solves the continuity and momentum equations in fully coupled form. Owing to these features, it easily permitted such full-scale computations. In Eça and Hoekstra (1996), the flow around tanker sterns at model and full scale were shown, including grid refinement studies indicating a good grid independence.

In a study on form factor scale effects in 2008, double-body flow computations have been made with this code for some standard test cases at model and full scale (Raven et al. 2008). One example shown was the Hamburg Test Case, a product carrier. We obtained the following form factors relative to the friction values from the ITTC'57 model-ship correlation line: $1+k_{\text{model}}=1.14$, $1+k_{\text{ship}}=1.22$, which shows a significant difference. Similar form factor increases had already been obtained for several other ships. Therefore, is the form factor method (assuming equality of the form factor) invalid?

However, we need to realise that the scale effect on the form factor depends on the plate friction line that is used; as Eq. (3) shows. Table 1 shows that the marked increase of $1+k$ from model to ship occurs for the two most popular friction lines, ITTC'57 and Schoenherr, but much less so for the more modern friction lines, from Grigson and Katsui. Therefore, how can we decide on the scale effect of $1+k$?

A plausible answer was obtained as follows. We want to know whether the viscous resistance coefficient of a ship is proportional to that of a flat plate over the Re range. Therefore, we compare the computed Cv value for the ship with that for a flat plate, computed with the same code and the same turbulence model. Different turbulence models do give somewhat different results, but that influence should largely be eliminated in this way. To this end, we use the "numerical friction lines" (Eça and Hoekstra 2008) that had been derived by very careful RANS computations for flat plates, using the same PARNASSOS code and several turbulence models.

Table 1 shows that relative to the numerical flat-plate friction line for the same turbulence model (Menter's $k-\sqrt{k}L$ model in this case), the form factor is almost equal for model and full scale; supporting the validity of the form factor method. This conclusion has been confirmed for many other ships, although exceptions occur. At the same time, this result, and the comparison with other flat-plate friction lines, suggests that the ITTC'57 line, when plotted against log(Re), has a too large slope. The flat-plate friction lines from Grigson and Katsui are a lot closer to the numerical friction lines and lead to a more constant form factor.

3.3 Lessons learnt

Therefore, from this and other cases, we conclude:

That the form factor concept itself is found largely valid: CFD computations indicate a good proportionality of the viscous resistance of a ship hull form, with the frictional resistance of a flat plate—both being computed by the same code and the same turbulence model; unless significant flow separation occurs;

That the same is true if one of the modern friction lines is used, but not the ITTC 57 or Schoenherr line;

That using a fixed form factor together with the ITTC 57 line (i.e. the method formerly recommended) leads to a prediction of full-scale viscous resistance that is significantly too low. This systematic underestimation was implicitly compensated by a part of the correlation allowance, but in view of the variables used in the expression for that allowance, that compensation could only be approximate.

For MARIN's model-to-ship extrapolation procedure, this study and later checks have led to the replacement of the ITTC'57 line by the Grigson line (along with a complete revision of the correlation coefficients). Besides, form factors are now always computed from double-body viscous-flow computations using PARNASSOS; and as a check, this is always done both for model and for full scale, such that also for cases with deviating scale effects, the right ship viscous resistance is estimated.

More recently, extensive studies have been done by Korkmaz (2020), which confirmed that a computational determination of the form factor is as accurate and often more practical than the experimental determination. Also, he has again derived numerical friction lines for various turbulence models, and it was demonstrated for an example that using those lines removes the clear underestimation of the full-scale viscous resistance found with the ITTC'57 line. Moreover, the combination of computed form factors with

numerical friction lines led to a reduced scatter of correlation coefficients for a large trial database. In a joint study of many institutes worldwide (Korkmaz et al. 2021), similar conclusions were reached. Thereby, this careful and comprehensive research has given support to a proposed revision of the recommended model-to-ship extrapolation procedure by the ITTC, using this 'Combined CFD/EFD method' as an option.

Therefore, in this example, the use of CFD has answered some of the classical questions in experimental ship hydrodynamics; confirming the validity of the form factor concept, indicating the replacement of the plate friction line; and improving the accuracy of predictions for cases with flow separation or other special scale effects.

4 Shallow-water effects on ship resistance

4.1 Introduction

The third example concerns the effect of shallow water on the flow and resistance; both in model tests and at full scale. Around 2006, it was reported to us that ships in shallow water were sometimes running significantly faster than had been predicted based on shallow-water model tests. Several studies have then been done to clarify and remove the causes of this. Up to that moment, shallow-water tests were essentially analysed like deep-water tests; and predictions made either by a Froude extrapolation, or by a form factor extrapolation. Some empirical estimation methods for shallow-water effects on resistance or power had been published; such as the methods by Schlichting (1934) and Lackenby (1963). Besides, some theoretical results were available, which only addressed the effect on the wave resistance (Kirsch 1966). As we know now, some of these papers have led to misunderstanding.

4.2 Tank width effects

Our first suspicion was that the limited width of the shallow-water model basin (while 16 m at MARIN) perhaps increased the model resistance and thus could cause the predictions (for shallow water of unlimited width) to be pessimistic. Tentatively, the measured resistance curve was shifted to a higher speed based on the overspeed (return flow) found from Kreitner's method (Kreitner 1934). This correction, however, appeared too large, incidentally resulting in a lower estimated resistance curve in shallow water than in deep water.

In Kreitner's method, it is assumed that the overspeed next to the model is uniformly distributed over the channel cross-section. The actual distribution has been calculated for various channel dimensions and ship speeds, using the potential flow solver RAPID. Figure 5 shows the crosswise distribution of the overspeed u as a fraction of the ship speed V, next to the ship's midship section, at the free surface. The different lines are for deep water, for shallow water of infinite width, and for some channels of equal depth but different width b. The narrower the channel, the higher the overspeed. Clearly the overspeed u/V is nonuniform, highest close to the ship and decreasing with distance. But remarkably, the overspeed increase $\Delta u/V$ due to the channel walls, compared to that in shallow water of infinite width, is fairly uniform: the line for 'shallow, wide' seems just shifted upwards. This fact was just observed owing to some simple computational work.

This then led to a new formulation of the channel effect (Raven 2019a). The ship's midship section A_m is an obstruction to the flow; the overspeed next to it must therefore carry an excess volume flux $A_m.V$. In a channel of width b, all this excess flux must be transported through the limited channel cross-section; but in shallow water of infinite width, there is also an overspeed at locations further from the ship, $y > b/2$ (i.e. outside the channel wall position) which carries a part of the required excess flux, Q_{out}. The overspeed increase $\Delta\gamma = \Delta u/V$, supposed uniform over the channel cross-section, must be such that it compensates this part of the excess flux. But this overspeed increase also leads to a lowering of the water level and resulting increase of the sinkage of the ship, thereby a further reduction of the available channel cross-section. Evaluating all this, we get a 3rd degree algebraic equation for $\Delta\gamma$, similar to but different from Kreitner's equation:

$$\Delta\gamma\left(1-\beta+\frac{1}{2}Fr_h^2(1-3\overline{\gamma}^2-3\overline{\gamma}\Delta\gamma-\Delta\gamma^2)\right)=\frac{Q_{out}}{VA_C} \tag{4}$$

in which β is the blockage, A_C is the channel cross-section, and $\overline{\gamma}$ is the overspeed ratio in shallow water of infinite width, averaged over the width of the channel. To solve this equation, we need Q_{out} and $\overline{\gamma}$, which are derived from a single shallow-water calculation using RAPID for one relevant speed. Then for each model speed we solve for $\Delta\gamma$. As Fig. 5 shows, the resulting estimate of the overspeed in a channel is in good agreement with the actual computed distribution, up to near the critical channel speed. From this $\Delta\gamma$, for each model speed a speed shift is derived which is applied to the measured resistance curve. Thereby, the resistance measured in the model basin for a speed V_{tank} is supposed to be valid for a slightly higher speed V_{shallow} in shallow water of equal depth but unlimited width. Besides, a correction is applied to the measured sinkage of the model.

Applying this correction for the limited tank width has been found to be absolutely essential to determine the true water depth effects (Raven 2019b). The tank width effect

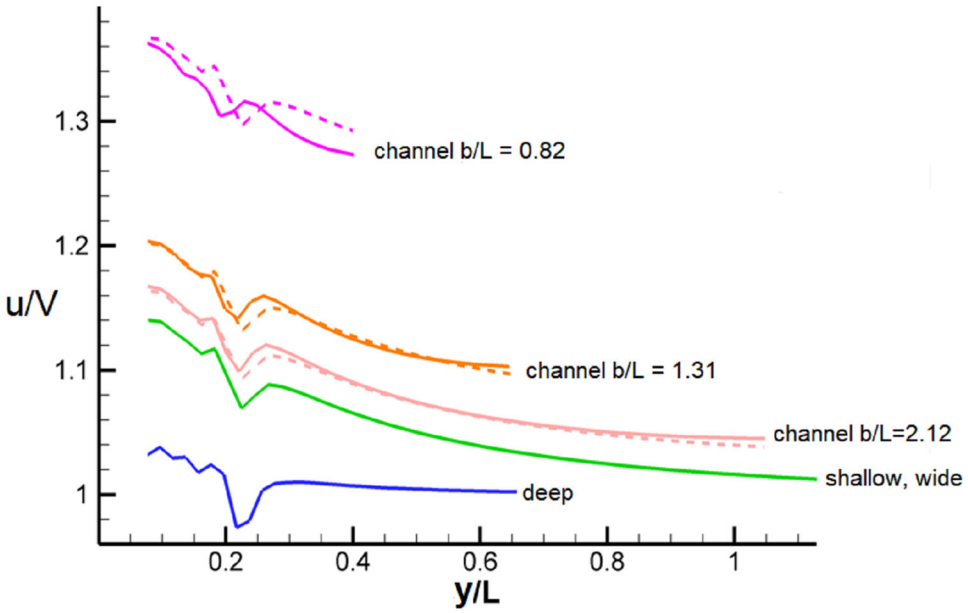

Fig. 5 Distribution of overspeed u as a fraction of ship speed V, next to the ship against distance from centreplane, at the midship section, at the free surface; in deep water, shallow water, and shallow channels of same depth. b = channel width, L is ship length. Series 60. $Cb = 0.60$, Froude number $Fr = 0.183$, water depth 0.082 L. Full lines: computed distribution; dashed lines: approximation $\Delta\gamma$ from Eq. (4) added to shallow-water curve

causes a resistance increase that grows quickly for decreasing water depth. Therefore, without such a correction, the apparent water-depth effect can easily be doubled. It is very likely that older empirical estimates for water-depth effects on resistance or sinkage have strongly been affected by the limited tank width used.

4.3 Model-to-ship extrapolation

Applying this tank-width correction to the model-test data reduced the overestimation of the full-scale resistance, but did not entirely remove it. Therefore, in a next study, the scale effects in the viscous resistance for ships in shallow water have been computed. Again, double-body flow RANS computations have been done using the PARNASSOS code (Hoekstra 1999; Van der Ploeg et al. 2000) for several ships, each in a range of water depths and for model and full scale. Thus, a clear picture was obtained of the shallow-water effect on viscous flow and resistance, and on its scale effect (Raven 2012).

Regarding the viscous resistance, we best plot the results as Cv/Cv_{deep} against T/h, in which T is the ship's draft and h is the water depth (Fig. 6). This figure includes not only computations done for this study, but also a collection of results from computations in practical projects, covering a variety of ships; plus a set of experimental data from Millward (1989). We observe that for $T/h < 0.5$–0.6, the relative increase of the viscous resistance (or form factor) for all cases available is in a rather narrow band. In this regime, the change of the streamline pattern over the hull is rather limited; but due to the lower pressure along the midbody in shallow water, pressure gradients at fore and aftbody are increased. The precise hull form does not matter much for the resistance increase here, and also the model and full-scale increases are nearly equal. The mean line plotted is the relation

$$Cv/Cv_{\text{deep}} = 1 + 0.57(T/h)^{1.79}. \tag{5}$$

However, in the shallower regime $T/h > 0.5$, there is a larger change of the streamline pattern over the hull. The proximity of the bottom of the waterway prevents part of the flow passing under the hull and forces the streamlines over the hull to follow a more horizontal path, rather following waterlines. This results in a larger apparent hull fullness, and still larger pressure gradients possibly leading to flow separation. In this regime, there is a larger dependence on the hull form, and also a larger difference between model and full scale.

This also tells directly how shallow-water model tests need to be analysed to get a full-scale prediction:

- first, the measured resistance curve needs to be corrected for tank width effects;
- next, the model resistance can be extrapolated to full scale using a water-depth dependent form factor; or a deep-water form factor multiplied by the mean line value shown in Fig. 6;
- if, however, T/h > 0.5, larger form factor scale effects can occur and it is safer to compute the viscous resistance coefficient in shallow water both for the model and for the ship, by simple double-body RANS calculations; and use these in the model-to-ship extrapolation.

Raven (2019b) gives an example of how large the differences can be due to these steps. The procedure described is

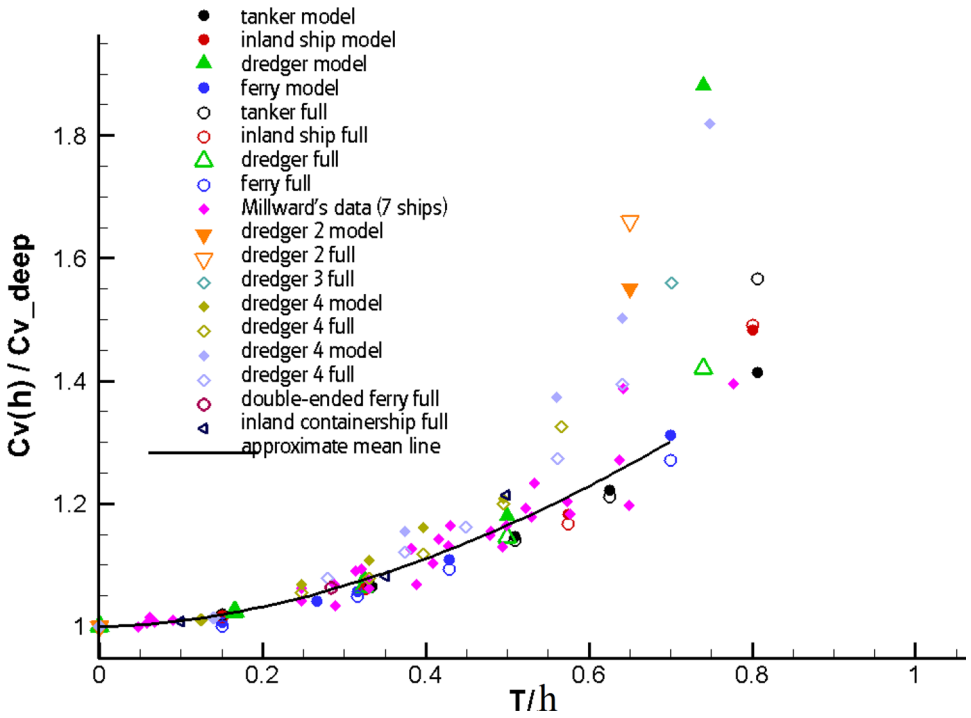

Fig. 6 Computed relative increase of viscous resistance coefficient in shallow water, for various ships and models (Raven 2016). Horizontal axis is ratio of ship draft to water depth, vertical axis is relative increase of viscous resistance coefficient in shallow water

being used at MARIN since 2012 and has much improved the prediction of required power of a ship in shallow water based on model tests.

4.4 A shallow-water trial correction method

With some additional work (Raven 2016), the same research led to what is now called the 'Raven shallow-water correction', a simple correction method for incipient shallow-water effects in full-scale speed trials (ITTC 2017a, b; Raven 2022). If the contractual speed for a new ship is specified for deep water, but the trials have been performed in a slightly limited water depth, a correction may be applied. This correction uses the mean line shown in Fig. 6 for the increase of viscous resistance, along with considerations on the change of the sinkage, wave resistance and propulsive efficiency. The set of simple empirical relations, derived using computational data, permits to estimate limited effects of shallow water on the resistance, for model and ship alike. It has now been accepted by the International Towing Tank Conference as a standard correction procedure, replacing the formula from Lackenby (1963).

Figure 7 illustrates what we learned in the process. It shows how, from a deep-water resistance curve for a ferry model, we estimate the shallow-water resistance curve (the blue dot-dash line) for $T/h = 0.46$, by adding the two components of the shallow-water correction: the change of viscous resistance, and the additional change of resistance due to the increased sinkage in shallow water. However, to estimate what would be measured in the model basin, we apply the speed shift for the tank width effect, from the method of Sect. 4.2, and get the red line. The black markers represent the actually measured points, which are in very good agreement with the estimates. The slight deviation at higher speeds can be attributed to the (disregarded) shallow-water effect on wave resistance that sets in around $\mathrm{Fr}_h = 0.70$ (15.4 kn in this case), outside the limit of applicability of the method. It is also clear that, if the tank width effect is not corrected for, the effect of shallow water seems much larger than it really is.

Therefore, not only we have derived some simple models based on the computed data but also we gained understanding: the difference in measured model resistance in shallow and deep water, which formerly just had to be taken for granted, can now be decomposed into its separate contributions, providing a clear view of what physically is taking place. Here again, some of the classical problems in steady ship hydrodynamics could be solved using today's computational methods.

5 Other challenges and unsolved problems

In ship hydrodynamics, even for the familiar resistance and propulsion field, there are still several unsolved problems, and subjects for which more information or validation is desired and could well be obtained from computational results. We mention a few.

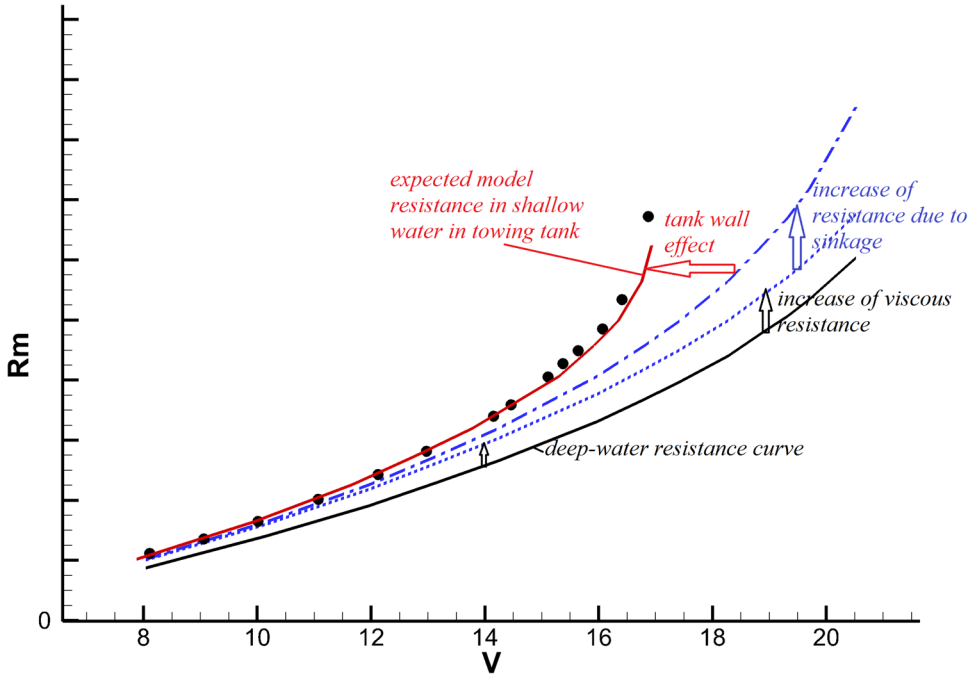

Fig. 7 Decomposition of difference between shallow-water and deep-water model resistance curve. The components are derived from the empirical shalllow-water correction, and the tank width correction. Black markers are actual measurements in shallow-water model basin. Model of ferry with $T = 6$ m, in water depth 13.1 m. Model resistance in N, against corresponding speed for full-scale ship in knots

The scale effect on the effective wake fraction (Taylor wake) plays an important role in the full-scale power and propeller RPM prediction based on model tests. Currently used approximations are very simple and possibly not always adequate. Computational studies are required. This requires a RANS solver for the hull flow, coupled with a propeller model, either by RANS or by a boundary element model for the propeller. In this way, a validation of the simple relations now used can be carried out, and perhaps a better model can be derived.

Scale effects on propeller characteristics (Kt, Kq) play a role in the full-scale predictions, and a way to correct for them is included in standard model-to-ship extrapolation methods. But usually these corrections are based on just the drag scale effect due to friction on the propeller blades, and disregard the scale effect on the lift. Improvement by computational studies should be possible, and work is being done on this subject. A topic of importance here is the occurrence of laminar areas and transition on the propeller blades at model scale. Predicting transition using CFD is a subject of development, perhaps not yet sufficiently mature to extract the required scaling information.

Several other subjects for which CFD studies can clarify scale effects, or for which CFD computations can be used as part of a full-scale prediction based on model tests, are discussed in (ITTC 2021). Besides, computational tools can contribute to our insight in hydrodynamics and design trends on several other points.

Thrust deduction affects the required power of a ship. Perhaps, more attention for its dependence on the hull form could help reducing that power. It can fairly easily be computed using a RANS solver coupled to a propeller model or body-force disk; and experimentation with hull forms should provide helpful design trends. As thrust deduction and effective wake tend to show similar variations but with opposite effect on required power, both should be computed and the effect on overall propulsive efficiency estimated.

With today's free-surface RANS codes, a study of wave/viscous interaction effects is possible. Viscous and scale effects on stern wave making exist, and their importance depends strongly on the case. Computational studies we have done so far did not yet lead to a full picture of the physics and design trends. Possibly, there would be room for further improvement of hull form designs if we would have a better understanding of the interaction effects and their meaning for ship resistance.

In all cases, it is essential that the CFD work is sufficiently reliable and numerically accurate, which is not evident for the more complicated subjects. But also it is important to realise that for some hydrodynamic problems CFD cannot yet provide a solution without further modelling and fundamental work. We mention a few examples.

The first is the effect of wave breaking on the trailing wave system and flow, and thereby on ship resistance and radiated wave height. While small amounts of breaking seem to mean little for ship resistance, for faster and fuller vessels it can be of importance. So far, trustworthy computational predictions with RANS codes seem absent for breaking ship waves. In Raven (2021), computed results for the 'Duncan foil' are

analysed, and it is shown that the wave dissipation by breaking in predictions by a Volume of Fluid RANS code is caused by numerical artefacts connected with the treatment of the interface, and deviates strongly from the physics. Therefore, in this case, computational work is not likely to provide a solution in a short term.

In some publications, resistance reduction by air lubrication is being computed using Volume of Fluid RANS codes. However, the single-fluid model used in such codes is likely to have a completely different effect on the boundary layer, turbulence and frictional resistance than a real flow with air bubbles. Therefore, unless extensive validation shows the opposite, the computational results should not be trusted.

For the effect of a given ship hull roughness and fouling on the flow and resistance, CFD models are all based on the use of an equivalent sand-grain roughness height. The latter can be approximately related with an Average Hull Roughness in case of a newly painted ship (Eça et al 2021), but relating any real-life roughness and fouling with an equivalent sand-grain roughness is a far more complicated problem. This is a 'missing link' for the application, but progress on a better modelling is being made (Chung et al 2021).

Therefore, a further advance of the knowledge on steady ship hydrodynamics can well be obtained from computational work, for several subjects but not for all.

6 Conclusions

The three examples discussed were meant to illustrate how a quick advance of the science of ship hydrodynamics, even for its most classical field (resistance and power), can be achieved by dedicated studies using CFD or other computational tools. The focus needed is on understanding the physics, and using that to understand design trends or to set up simple models. This is a different focus than to aim at the most complete or advanced prediction tool, although of course a good numerical accuracy is essential. The present paper is meant to advocate such work, as an important step towards further improvement of ship and propeller designs.

The first example given showed how, based on inspection and analysis of results of free-surface potential flow computations, and being aware of simplified ship wave-making theories, a conceptual model could be deduced that helps understanding the mechanism of ship wave making. The same insights are still used in the context of CFD-based hull form optimisation.

The second example addressed the scaling of viscous resistance. Double-body RANS computations and numerical plate friction lines quickly resolved some questions that before could hardly be disentangled; confirming the validity of the form factor scaling method, but just when based on a proper plate friction line.

The third example showed how by straightforward computational work, using both potential flow and RANS codes, the effect of the towing tank width in shallow-water model testing could be quantified and eliminated, the model-to-ship extrapolation was revised, a shallow-water trial correction could be derived and insight was collected on the contributions to the shallow-water effect on resistance.

Of course, while all three examples were largely taken from our own research done at MARIN, many similar developments have been done elsewhere and much progress has been made. On a personal note, in my 43 years involvement in the development and application of computational methods for ship resistance and flow, such use of methods to extend the hydrodynamics knowhow has been a main theme. With the present paper, I am hoping to inspire others to continue contributing to the knowledge of ship hydrodynamics and hydrodynamic ship design by exploiting the capabilities of today's computational tools.

Acknowledgements Most of the research described in this paper has been funded by the Dutch Ministry of Economic Affairs over the years.

References

Baba E, Takekuma K (1975) A study on free-surface flow around bow of slowly moving full forms. J Soc Nav Archit Jpn 137

Chung D, Hutchins N, Schultz MP, Flack KA (2021) Predicting the drag of rough surfaces. Annu Rev Fluid Mech 53:439–471

Dawson CW (1977) A Practical Computer Method for Solving Ship-Wave Problems. In: Proceedings of 2nd International Conference Numerical Ship Hydrodynamics, Berkeley, USA

Eça L, Hoekstra M (1996) Numerical Calculations of Ship Stern Flows at Full-Scale Reynolds Numbers. In: Proceedings of 21st Symposium Naval Hydrodynamics, Trondheim, Norway

Eça L, Hoekstra M (2008) The numerical friction line. J Mar Sci Technol 13:328–345

Eça L, Starke AR, Kerkvliet M, Raven HC (2021) On the contribution of roughness effects to the scaling of ship resistance, MARINE 2021 Conference

Hoekstra M (1999) Numerical simulation of ship stern flows with a space-marching Navier Stokes method, Dissertation. Delft University of Technology, Delft

ITTC (2017a) Report of Specialist Committee on Performance of Ships in Service. In: Proceedings of 28th ITTC, Wuxi, China, International Towing Tank Conference (ed)

ITTC (2017b) Preparation, conduct and analysis of speed/power trials. Appendix K, 'Raven shallow-water correction. ITTC Recommended procedures and guidelines 7.5-04-01-01.1

ITTC (2021) Report of the specialist committee on CFD and EFD combined methods. In: 29th International Towing Tank Conference

Janson CE (1997) Potential-flow panel methods for the calculation of free-surface flows with lift, Dissertation, Chalmers University, Gothenburg, Sweden

Jensen G (1988) Berechnung der Stationären Potentialströmung um ein Schiff unter Berücksichtigung der Nichtlinearen Randbedingung an der Wasseroberfläche, Dissertation, University of Hamburg, IfS Bericht, p 484

Kirsch M (1966) Shallow water and channel effects on wave resistance. J Ship Res 10–3:164–181

Korkmaz KB (2020) Improved power predictions of ships using combined cfd/efd methods for the form factor, licentiate thesis. Chalmers University of Technology, Gothenburg

Korkmaz KB, Werner S, Sakamoto N, Queutey P, Deng G, Yuling G, Guoxiang D, Maki K, Ye H, Akinturk A, Sayeed T, Hino T, Zhao F, Tezdogan T, Demirel YK, Bensow R (2021) CFD based form factor determination method. Ocean Eng 220:108

Kreitner J (1934) Über den Schiffswiderstand auf beschränktem Wasser. Werft Reeder Hafen 15–7:77–82

Lackenby H (1963) The effect of shallow water on ship speed. Shipbuilder marine engine builder. Wiley, New Jersey, pp 446–450

Larsson L, Raven HC (2010) Ship resistance and flow. Principles of naval architecture series. SNAME, New Jersey

Lighthill J (1980) Waves in fluids. Cambridge University Press, Cambridge, pp 404–409

Millward A (1989) The effect of water depth on hull form factor. Int Shipbuild Progr 36–407:283–302

Newman JN (1976) Linearized wave resistance theory. In: Proceedings of International Seminar on Wave Resistance, Tokyo/Osaka, Society Naval Arch. Japan

Raven HC (1988) Variations on a theme by Dawson. In: Proceedings of 17th Symposium Naval Hydrodynamics, Den Haag, Netherlands

Raven HC (1992) A practical nonlinear method for calculating ship wavemaking and wave resistance. In: Proceedings of 19th Symposium Naval Hydrodynamics, Seoul, South-Korea

Raven HC (1996) A solution method for the nonlinear ship wave resistance problem. Dissertation, Delft University Technology, Delft, Netherlands

Raven HC (2010) Validation of an approach to analyse and understand ship wave making. J Mar Sci Technol 15:331–344

Raven HC (2012) A computational study of shallow-water effects on ship viscous resistance. In: Proceedings of 29th Symposium Naval Hydrodynamics, Gothenburg, Sweden

Raven HC (2014) Analysing numerical flow computations for practical ship hull form design, invited lecture. In: 30th Symposium Naval Hydrodynamics, Hobart, Australia

Raven HC (2016) A new correction procedure for shallow-water effects in ship speed trials. In: Proceedings of 13th International Symposium on Practical Design of Ships (PRADS), Kopenhagen, Denmark

Raven HC (2019a) A method to correct shallow-water model tests for tank wall effects. J Mar Sci Technol 24(2):437–453

Raven HC (2019b) Shallow-water effects in ship model testing and at full scale. Ocean Eng 189:106

Raven HC (2021) Credibility of wave breaking computations by Volume of Fluid RANS codes. In: 23rd Numerical Towing Tank Symposium, Mülheim/Ruhr, Germany

Raven HC (2022) A correction method for shallow-water effects on ship speed trials. The 'Raven shallow-water correction', Report 98800-1-RD, MARIN, https://www.marin.nl/en/publications/a-correction-method-for-shallow-water-effects-on-ship-speed-trials

Raven HC, Scholcz TP (2017) Wave Resistance Minimisation in Practical Ship Design. Proceedings of VII International Conference on Computational Methods in Marine Engineering (MARINE2017), Nantes, France

Raven HC, Van der Ploeg A, Starke AR (2008) Towards a CFD-based prediction of ship performance: progress in predicting full-scale resistance and scale effects. Int J Marit Eng, Trans RINA Part A 150–A4:31–42

Schlichting O (1934) Schiffswiderstand auf beschränkter Wassertiefe-Widerstand von Seeschiffen auf flachem Wasser. STG Jahrbuch Vol. 35

Sharma SD, Naegle JN (1970) Optimization of bow bulb configurations on the basis of model wave profile measurements, Report 104, Department of Naval Arch. Marine Engineering, University of Michigan, USA

Van der Ploeg A, Eça L, Hoekstra M (2000) Combining accuracy and efficiency with robustness in ship stern flow calculation. In: Proceedings of 23rd Symposium Naval Hydrodynamics, Val de Rueil, France